Available online at www.sciencedirect.com

ScienceDirect

Advances in Space Research 69 (2022) 4169–4178

ADVANCES IN SPACE RESEARCH
(a COSPAR publication)

www.elsevier.com/locate/asr

Note on the analytical integration of circumterrestrial orbits

Martin Lara

Scientific Computing and Technological Innovation Center – University of La Rioja, C/ Madre de Dios, 53, ES-26006 Logroño, Spain
Space Dynamics Group – UPM, Plaza del Cardenal Cisneros, 3, ES-28040 Madrid, Spain

Received 16 October 2021; received in revised form 20 February 2022; accepted 3 April 2022
Available online 9 April 2022

Abstract

The acclaimed merits of analytical solutions based on a fictitious time developed in the 1970's were partially overvalued due to a common misuse of classical analytical solutions based on the physical time that were taken as reference. With the main problem of the artificial satellite theory as a model, we carry out a more objective comparison of both kinds of theories. We find that the proper initialization of classical solutions notably balances the performance of the two distinct approaches in what respects to accuracy. Besides, extension of both kinds of satellite theories to higher orders show additional pros and cons of each different perturbation approach, thus providing complementary information to prospective users on which kind of analytical solution may better support their needs.

Keywords: Circumterrestrial orbits; Analytical solutions; In-track errors; Fictitious time; Extended phase space

1. Introduction

The advent of the perturbation theories of Kozai (1959) and Brouwer (1959) made a breakthrough in the analytical computation of circumterrestrial orbits. Both theories were computed in closed form of the eccentricity, thus extending their range of application from the lower eccentricities to highly elliptic orbits, and successfully included the effects of higher degree zonal harmonics of the geopotential as well as the second order effects of the dominant, zonal harmonic of the second degree —customarily denoted J_2. Brouwer and Kozai's analytical solutions are given in the form of collections of truncated power series of J_2 with time as the argument. Several of these series represent the secular terms of the solution, which are expected to provide the average orbit evolution, and the remaining series comprise the periodic corrections that are needed for computing the ephemeris. In the original proposals of Kozai and Brouwer, the former were accurate up to the second order of J_2 effects, whereas the later were truncated to $\mathcal{O}(J_2)$.

A crucial point in the use of these kinds of truncated power series is the initialization of the constants of the theory (Cain, 1962; Walter, 1967; Ustinov, 1967; Eckstein and Hechler, 1970; Gaias et al., 2020). In particular, the accurate determination of the "mean" mean motion —that is, the mean motion in mean (or secular) variables— is mandatory to obtain the in-track error that would be expected from the truncation of the secular terms. This point was clearly highlighted by the developers of perturbation solutions (see remarks in Kozai, 1962). However, it created some confusion among users, who reported unexpected along-track errors in the propagation of initial conditions when Brouwer's theory was compared with alternative available solutions (see Bonavito et al., 1969, and references therein). The trouble resulted from Brouwer's computation of the periodic corrections —which are needed for the initialization of the constants of the theory from given initial conditions— to a lower order than the one of the secular terms. On the other hand, this inac-

E-mail address: mlara0@gmail.com

https://doi.org/10.1016/j.asr.2022.04.007
0273-1177/

curacy did not happen when the value of the "mean" mean motion was known to the required accuracy by other means, like the usual fit to observations. Therefore, the problem was understood to be an inconsistency in the use of Brouwer's solution.

Increasing the truncation order of the periodic corrections to solve the inconsistency involves heavy additional analytical computations (Kozai, 1962; Deprit and Rom, 1970), which commonly discouraged users from their implementation. However, since the increased accuracy was fundamentally needed for the osculating to mean conversion of the semimajor axis, simple ways of patching Brouwer's solution were soon devised (Lyddane and Cohen, 1962). In this regard, the alternative proposed by Breakwell and Vagners (1970) is remarkable, because it does not require additional computations to those already carried out by Brouwer. Indeed, the smart use of the energy equation to calibrate the mean semimajor axis provided a computationally inexpensive way of reducing in-track errors to a comparable level of those in the radial and cross-track directions (see Lara, 2021a, for instance).

Conversely, because the accurate initialization of the mean semimajor axis is clearly associated with the correct treatment of the total energy, the pronounced loss of accuracy in the in-track direction does not happen to perturbation solutions formulated in the extended phase space, in which the total energy is one more integration variable (Scheifele, 1970; Scheifele, 1970; Stiefel and Scheifele, 1971). In this scenario, the analytical solution is advantageously computed in a fictitious-time scale, whereas the physical time is incorporated into the perturbation scheme as the conjugate coordinate of the total energy. In particular, the annoying complications introduced by the equation of the center when dealing with geopotential perturbations in closed form (Jefferys, 1971; Deprit, 1981; Metris, 1991; Ahmed, 1994; Lara, 2019a) are now totally avoided.

The merits of the extended phase space formulation in the implementation of an analytical orbit generator are unquestionable (Scheifele, 1981). However, assertions such that as the accuracy of first order analytical solutions based on this approach compare with traditional second order perturbation solutions based on the physical time (Scheifele and Graf, 1974) are true only when the latter is incorrectly initialized, and hence must be somewhat downgraded. To show that, we take the main problem of the artificial satellite theory as a demonstration model, and make an independent implementation of both kinds of theories. Needless to say that our implementation of the traditional one, based on the physical time, incorporates the calibration of the mean semimajor axis in the initialization part of the orbit theory. While we still found higher accuracy of the secular terms in the case of the fictitious-time approach, in no way does it reach the accuracy of a second-order traditional (correctly initialized) perturbation solution. In addition, we show that, due to the unavoidable truncation of the time equation, additional errors arise in the fictitious-time approach that are of comparable magnitude to the obtained position errors. Moreover, the need of inverting the time equation, or resorting to iterative procedures for finding the fictitious time corresponding to a given physical time (Bond, 1979), which is needed for usual ephemeris prediction, must also be taken as a shortcoming of the fictitious-time approach because it notably increases the computational burden of usual ephemeris evaluation.

To further assess the relative merits of each perturbation approach, we extended both kinds of satellite theories to the second order that is customarily used in accurate analytic ephemeris prediction programs (Coffey and Alfriend, 1984; Coffey et al., 1996). In the case of the extended phase space formulation, spurious higher-order terms are generated at each order of the perturbation algorithm, a fact that makes the series defining the analytical solution notably longer than those resulting from the traditional, physical-time approach. Therefore, a post-processing is mandatory to keep the length of the series comprising the perturbation solution based on the fictitious time of comparable size to those of the traditional solution based on the physical time.

2. Solution to the J_2-problem in the extended phase space

The topic of perturbation solutions of the artificial satellite problem using the traditional approach is satisfactorily covered in the literature. In particular, for the main problem, explicit expressions of higher-order solutions have been provided in different places (see Healy, 2000; Lara, 2019b; Lara, 2020, for instance). Therefore, we focus on the less studied formulation of perturbation solutions in the extended phase space, which, as customary nowadays, we recompute using the method of Lie transforms (Deprit, 1969) rather than the von Zeipel perturbation algorithm used in the original developments (Scheifele and Graf, 1974).

We approach the perturbation solution in the true anomaly Delaunay-similar elements (Scheifele, 1970; Scheifele, 1970; Floría, 1997). These elements are the action-angle variables of the unperturbed problem —the Kepler problem in the extended phase space, with the true anomaly as the independent variable— in which the complete Hamiltonian reduction of perturbed problems is naturally achieved. The fact that the Delaunay-similar elements are harmed by singularities is not at all of concern. Indeed, once the perturbation solution is computed, we can always reformulate it at our will in our preferred choice of singular or non-singular, canonical or non-canonical variables (Lyddane, 1963; Deprit and Rom, 1970).

2.1. The main problem in Delaunay-similar variables

The main problem admits a Hamiltonian formulation. Using polar variables, the Hamiltonian is written in the form (see Deprit and Ferrer, 1987, for instance)

$$\mathcal{H} \equiv \frac{1}{2}\left(R^2 + \frac{\Theta^2}{r^2}\right) - \frac{\mu}{r} + J_2 \frac{\mu}{r} \frac{R_\oplus^2}{r^2} P_2(s \sin\theta), \tag{1}$$

where $\mu, R_\oplus$, and J_2, are physical parameters that characterize the gravity field, and stand for the Earth's gravitational parameter, equatorial radius, and oblateness coefficient, respectively; r is the radius, R the radial velocity, the polar angle θ is commonly dubbed as the argument of the latitude, Θ is the total angular momentum (per unit mass), P_2 is the Legendre polynomial of degree 2, and $s \equiv \sin I$, with I denoting orbital inclination. The third component of the specific angular momentum $N = \Theta \cos I$ is an integral that stems from the axial symmetry of the main problem.

Hamiltonian (1) is conveniently formulated in the *extended phase space* (Poincaré, 1893; Stiefel and Scheifele, 1971) by adding the pair of variables $q = t$ and $Q = -\mathcal{H}$, and defining the new Hamiltonian $\mathcal{H}^* \equiv \mathcal{H} + Q$, which, therefore, is constrained to the manifold $\mathcal{H}^* = 0$. If, besides, we define a new time scale τ, such that $\mathrm{d}t = \Psi(r, \theta, R, \Theta, q, Q)\,\mathrm{d}\tau$, it can be checked that the Hamiltonian $\widetilde{\mathcal{H}} \equiv \mathcal{H}^*\Psi$ remains constant in the new time scale, and that the solution of the system governed by $\widetilde{\mathcal{H}}$ coincides with the system governed by $\mathcal{H}^*$ when the initial conditions for $\tau = 0$ are the same as the ones for $t = 0$ (Scheifele, 1970). In particular, the choice

$$\mathrm{d}t = \frac{r^2}{\Gamma(r, \theta, \Theta, N)}\,\mathrm{d}\tau, \tag{2}$$

allows us to replace Eq. (1) by

$$\widetilde{\mathcal{H}} \equiv \left[\frac{1}{2}\left(R^2 + \frac{\Theta^2}{r^2}\right) - \frac{\mu}{r} + J_2 \frac{\mu}{r} \frac{R_\oplus^2}{r^2} P_2(s \sin\theta) + Q\right]\frac{r^2}{\Gamma}, \tag{3}$$

the solutions of which only make sense in the manifold $\widetilde{\mathcal{H}} = 0$. Remark that the regularization in Eq. (2) is valid for any Γ as far as the new time scale τ remains monotonic. The same comment applies to the function Ψ.

When choosing

$$\Gamma = \frac{1}{2}\Theta\left\{1 + \left[1 + 2J_2 \frac{\mu}{r} \frac{R_\oplus^2}{\Theta^2} P_2(s \sin\theta)\right]^{1/2}\right\}, \tag{4}$$

which only differs from Θ on the order of J_2, the Hamiltonian (3) can be suitably formulated in the Delaunay-similar variables $(\phi, g, h, \lambda, \Phi, G, H, \Lambda)$, where ϕ is the true anomaly, g is the argument of the perigee, h is the right ascension of the ascending node, λ is the time element, Φ is related to the Keplerian energy, $G = \Theta, H = N$, and $\Lambda = Q$. They are computed from polar variables as follows (see Scheifele and Graf, 1974; Deprit, 1981; Floría, 1997; Ferrer and Lara, 2010, for details)

$$\Phi = 2(\Theta - \Gamma) + \frac{\mu}{(2Q)^{1/2}}, \tag{5}$$

$$p = \frac{1}{\mu}(2\Theta - \Gamma)^2, \tag{6}$$

$$e = \sqrt{1 - 2Qp/\mu}, \tag{7}$$

$$\cos\phi = \frac{1}{e}\left(-1 + \frac{p}{r}\right), \qquad \sin\phi = \frac{R}{e}\sqrt{\frac{p}{\mu}}, \tag{8}$$

$$u = 2\arctan\left(\sqrt{\frac{1-e}{1+e}}\tan\frac{\phi}{2}\right), \tag{9}$$

$$\lambda = q - \frac{\mu}{(2\Lambda)^{3/2}}(u - e\sin u - \phi). \tag{10}$$

In these variables, Hamiltonian (3) takes the form

$$\mathcal{F} \equiv \Phi - \frac{\mu}{\sqrt{2\Lambda}} - J_2 \frac{\mu}{r} \frac{R_\oplus^2}{\Gamma} \times \frac{1}{4}\left[2 - 3s^2 + 3s^2\cos 2(g + \phi)\right], \tag{11}$$

in which, now,

$$s^2 = 1 - \frac{H^2}{G^2}, \quad r = \frac{p}{1 + e\cos\phi}, \quad \Gamma = G - \frac{1}{2}\left(\Phi - \frac{\mu}{\sqrt{2\Lambda}}\right).$$

2.2. Perturbation approach

Due to the smallness of the Earth's J_2 coefficient, the complete Hamiltonian reduction of the main problem Hamiltonian (11) can be achieved, up to some truncation order, by the Lie transforms method. We assume that the reader is familiar enough with this perturbation method (see Deprit, 1969; Boccaletti and Pucacco, 2002; Lara, 2021b, for reference) and only provide the results.

In our approach, we adhere to the tradition and carry out the sequential elimination of short- and long-period terms (Brouwer, 1959; Scheifele and Graf, 1974). This is done analytically by changing first from original to prime variables, and then from prime variables to mean (double-prime) variables. The complete Hamiltonian reduction is then achieved by neglecting higher-order terms from the mean elements Hamiltonian, to obtain

$$\mathcal{F}'' \equiv \mathcal{F}''(-, -, -, -, \Phi'', G'', H'', \Lambda''). \tag{12}$$

The analytical solution is trivial in mean elements. Indeed, the Hamilton equations of Eq. (12) immediately show that the momenta are constant in mean elements

$$\Phi'' = \Phi_0'', \quad G'' = G_0'', \quad H'' = H, \quad \Lambda'' = \Lambda, \tag{13}$$

where H and Λ are integrals of the original main problem, whereas the angles evolve linearly with constant frequencies given by

$$n_\phi = n_\phi(\Phi_0'', G_0'', H, \Lambda) = \partial\mathcal{F}''/\partial\Phi'', \tag{14}$$

$$n_g = n_g(\Phi_0'', G_0'', H, \Lambda) = \partial\mathcal{F}''/\partial G'', \tag{15}$$

$$n_h = n_h(\Phi_0'', G_0'', H, \Lambda) = \partial\mathcal{F}''/\partial H'', \tag{16}$$

$$n_\lambda = n_\lambda(\Phi_0'', G_0'', H, \Lambda) = \partial\mathcal{F}''/\partial\Lambda''. \tag{17}$$

To avoid offending divisors in the perturbation series, the analytical solution is customarily formulated in the canonical set of non-singular Poicaré-similar elements (Scheifele, 1981). However, due to the axial symmetry of the main problem model, we find convenience in formulating the solution in a non-canonical set of variables that replaces the troublesome elements by the argument of the latitude $\theta = \phi + g$ and the semi-equinoctial elements defining the eccentricity vector in the orbital plane $C = e\cos g, S = e\sin g$. The solution in mean elements is thus

$$\lambda'' = \lambda_0'' + n_\lambda\tau, \tag{18}$$

$$\theta'' = \theta_0'' + (n_\phi + n_g)\tau, \tag{19}$$

$$C'' = C_0''\cos(n_g\tau) - S_0''\sin(n_g\tau), \tag{20}$$

$$S'' = S_0''\cos(n_g\tau) + C_0''\sin(n_g\tau), \tag{21}$$

$$h'' = h_0'' + n_h\tau, \tag{22}$$

and the original dynamics is recovered by plugging this solution into the transformation from mean to osculating elements, which in the current, Hamiltonian case is derived from a generating function.

We extended the solution of Scheifele and Graf (1974) to the second order. That is, the secular terms in Eqs. (18)–(22) are accurate to $\mathcal{O}(J_2^3)$ effects, whereas the periodic corrections are accurate only to $\mathcal{O}(J_2^2)$. Accordingly, the analytical solution comprises 33 perturbation series in addition to those defining the secular frequencies. Namely, 5×3 for the long-period corrections (first-order, second-order direct, and second-order inverse), and 6×3 for the short-period corrections (first-order, second-order direct, and second-order inverse). Remarkably, there is no need of integrating Eq. (2) to recover the physical time, which, on the contrary, due to the extended phase space formulation is obtained by making explicit q from Eq. (10).

Note that, due to the truncation of the periodic corrections, the initialization of the perturbation theory from a given set of initial conditions provides the needed constants in Eqs. (13)–(17) only up to $\mathcal{O}(J_2^2)$ effects, whereas the secular frequencies are expected to be accurate to the order of J_3^3. While this is an inconsistency in traditional perturbation theories, which need to be patched to avoid large in-track errors, we will see that this uneven truncation is not of concern in the extended phase space formulation.

2.3. First-order solution

The generating function of the short-period elimination is

$$\mathcal{W}_1 = -\tfrac{1}{8}\Gamma\tfrac{R_\oplus^2}{\rho^2}[(4-6s^2)e\sin\phi + 3es^2\sin(2g+\phi) + 3s^2\sin(2g+2\phi) + es^2\sin(2g+3\phi)], \tag{23}$$

where we defined the auxiliary variable

$$\rho = \Gamma\sqrt{p/\mu}.$$

Remarkably, Eq. (23) is formally the same as the first order term of the generating function of the elimination of the parallax transformation when it is written in Delaunay variables (cf. Lara et al., 2014).

Up to the first order, the transformation of the short-period elimination is computed as $\xi = \xi' + J_2\delta_{1,\xi}$, with ξ denoting any of the involved variables. The short-period corrections $\delta_{1,\xi}$ are obtained from the computation of the Poisson bracket $\{\xi, \mathcal{W}_1\}$, and reformulating the result in prime variables. The inverse transformation is $\xi' = \xi - J_2\delta_{1,\xi}$ where now $\delta_{1,\xi}$ is written in the original, non-primed variables.

For the long-period elimination we obtain the first order generating function

$$\mathcal{V}_1 = \Gamma\frac{R_\oplus^2}{\rho^2}\frac{3}{32}\frac{1}{\Delta}\left[15s^2 - 14 + 12(s^2-1)\delta\right]s^2e^2\sin 2g, \tag{25}$$

which must be written in the prime variables. In Eq. (25) we abbreviated

$$\Delta = 3(5s^2-4) + 6(s^2-1)\delta + 2(3s^2-2)\upsilon, \tag{26}$$

and introduced the auxiliary, non-dimensional functions

$$\delta = -1 + \Gamma/G, \qquad \upsilon = -1 + \rho/p, \tag{27}$$

which are $\mathcal{O}(J_2)$, and hence produce a small displacement of similar magnitude in the critical inclination value, which now happens for $\Delta = 0$. That is, $\sin I = \sqrt{4/5} + \mathcal{O}(J_2)$. The first-order transformation to mean (double-prime) elements is computed like before. Thus, $\xi' = \xi'' + J_2\delta'_{1,\xi'}$, where the long-period corrections $\delta'_{1,\xi'}$ are obtained computing the Poisson bracket $\{\xi', \mathcal{V}_1\}$, and reformulating the result in the double-prime variables. Analogously, $\xi'' = \xi' - J_2\delta'_{1,\xi'}$ with $\delta'_{1,\xi'}$ now written in prime variables.

The secular frequencies of the first order theory are obtained from the Hamilton equations of the secular Hamiltonian

$$\mathcal{F}'' = \Phi - \frac{\mu}{\sqrt{2\Lambda}} + \sum_{m\geq 1}\frac{J_2^m}{m!}\mathcal{F}_m, \tag{28}$$

where

$$\mathcal{F}_1 = \Gamma\frac{R_\oplus^2}{\rho^2}\frac{1}{4}(3s^2-2), \tag{29}$$

and

$$\mathcal{F}_2 = \Gamma\tfrac{R_\oplus^4}{\rho^4}\tfrac{1}{64}[4(15s^4 - 6s^2 - 4) + 3(5s^4 + 8s^2 - 8)e^2 + 24s^2 \times(2e^2+3)(s^2-1)\delta - 2(e^2+1)(15s^4 - 24s^2 + 8)\upsilon], \tag{30}$$

are written in mean (double-prime) variables.

2.4. Second-order solution

The second order generating function takes the form

$$
\begin{aligned}
\mathcal{W}_2 = {} & \Gamma\tfrac{R_\oplus^4}{p^4}\tfrac{1}{3840}\{60[45s^4+72s^2-80+168s^2(s^2-1)\delta-4\\
&\times(33s^4-48s^2+16)\upsilon]e\sin\phi+360[(5s^2-4)s^2+4s^2\\
&\times(s^2-1)\delta]e^2\sin 2\phi-90[225s^2-206+168(s^2-1)\delta\\
&+4(3s^2-2)\upsilon]s^2e\sin(2g+\phi)-120\{39s^2-38+36(s^2\\
&-1)\delta-2(3s^2-2)\upsilon+2e^2[3s^2-4+6(s^2-1)\delta-(3s^2\\
&-2)\upsilon]\}s^2\sin(2g+2\phi)+10[75s^2-42-24(s^2-1)\delta\\
&+28(3s^2-2)\upsilon]s^2e\sin(2g+3\phi)+30[15s^2-14+12(s^2\\
&-1)\delta]s^2e^2\sin(2g+4\phi)+45(4\upsilon+5)s^4e\sin(4g+3\phi)\\
&+45[2(\upsilon+1)+(2\upsilon+3)e^2]s^4\sin(4g+4\phi)\\
&+9(4\upsilon+5)s^4e\sin(4g+5\phi)\}.
\end{aligned}
\tag{31}
$$

Now

$$
\xi=\xi'+J_2\delta_{1,\xi}+\frac{1}{2}J_2^2\delta_{2,\xi},
$$

where $\delta_{2,\xi}$ is obtained after reformulating in prime variables the result of $\{\{\xi,\mathcal{W}_1\},\mathcal{W}_1\}+\{\xi,\mathcal{W}_2\}$. For the inverse transformation,

$$
\xi'=\xi-J_2\delta'_{1,\xi}+\frac{1}{2}J_2^2\delta'_{2,\xi},
\tag{33}
$$

where $\delta'_{2,\xi}$ is no longer the opposite of $\delta_{2,\xi}$, but the result, in the original variables, of $\{\{\xi,\mathcal{W}_1\},\mathcal{W}_1\}-\{\xi,\mathcal{W}_2\}$.

The secular frequencies of the second-order theory are computed from the Hamiltonian (28), which is now complemented with the third-order term

$$
\mathcal{F}_3=\Gamma\frac{R_\oplus^6}{p^6}\frac{3}{2^{10}}\frac{1}{\Delta^2}\sum_{k=0}^{2}\sum_{j=0}^{4}\sum_{i=0}^{4-j}q_{k,i,j}(1+\delta)^i(1+\upsilon)^j e^{2k},
\tag{34}
$$

where the coefficients $q_{k,i,j}$ are given in Table 1.

The second-order term of the generating function of the transformation of the long-period elimination is

$$
\begin{aligned}
\mathcal{V}_2 = {} & \Gamma\tfrac{R_\oplus^4}{p^4}\tfrac{3}{2^{10}}\tfrac{1}{\Delta^3}\sum_{l=1}^{2}\sum_{k=0}^{2-l}\sum_{j=0}^{4}\sum_{i=0}^{4-j}b_{l,k,i,j}\\
&\times(1+\delta)^i(1+\upsilon)^j e^{2k+2l}s^{2l}\sin 2lg,
\end{aligned}
\tag{35}
$$

where the inclination polynomials $b_{l,k,i,j}$ are listed in Table 2. The transformation of the long-period elimination is obtained analogously to Eq. (32) —resp. (33)— and following formulas, replacing corresponding functions and variables by those of the long-period case.

Remarkably, at this order there is an explosion in the number of terms of the transformation of the long-period elimination. This is clearly shown by comparison with Brouwer's 2nd order generating function of the long-period elimination, which takes the much simpler form

$$
\mathcal{V}_2^*=G\frac{R_\oplus^4}{p^4}\frac{1}{2^{10}}\frac{1}{\tilde{\Delta}^2}\sum_{j=1}^{2}\frac{(1+\eta)^{j-2}}{\tilde{\Delta}^{j-1}}\sum_{i=0}^{3j^*}b_{j,i}\eta^i e^{2j}s^{2j}\sin 2jg,
\tag{36}
$$

where $\eta=(1-e^2)^{1/2}$, $\tilde{\Delta}=5s^2-4$, $j^*=(j \bmod 2)$, and

$$
\begin{aligned}
b_{1,0}&=-2(3975s^6-6870s^4+2928s^2+16),\\
b_{1,1}&=2(1425s^6-5370s^4+6288s^2-2320),\\
b_{1,2}&=-2(15s^2-14)(195s^4-388s^2+184),\\
b_{1,3}&=2(15s^2-14)(45s^4+36s^2-56),\\
b_{2,0}&=(15s^2-14)^2(15s^2-13).
\end{aligned}
\tag{37}
$$

Still, if third-order corrections are not of concern, after computing the second-order corrections stemming from Eq. (35), they can be notably simplified by making $\delta=\upsilon=0$. Other terms of the different series that compose the solution in the extended phase space are certainly amenable to analogous simplifications.

3. Accuracy tests

A number of tests has been conducted to check the accuracy of the analytical solution based on the fictitious time and compare it with the precision provided by the tradi-

Table 1
Inclination polynomials $q_{k,i,j}$ in Eq. (34); $c=(1-s^2)^{1/2}$.

i,j	$k=0$	$k=1$	$k=2$
0,0	$-72(2-3s^2)^3s^4$	$-4(2-3s^2)^3(41s^4-24s^2+8)$	$18(2-3s^2)^3s^4$
0,1	$-4(2-3s^2)^3(67s^4-24s^2+8)$	$-2(2-3s^2)^3(413s^4-432s^2+144)$	$54(2-3s^2)^3s^4$
0,2	$-32(2-3s^2)^3(15s^4-24s^2+8)$	$-4(2-3s^2)^3(513s^4-816s^2+272)$	$9(2-3s^2)^3s^4$
0,3	$-16(2-3s^2)^3(63s^4-120s^2+40)$	$-16(2-3s^2)^3(217s^4-360s^2+120)$	0
0,4	$-64(2-3s^2)^3(17s^4-24s^2+8)$	$-160(2-3s^2)^3(17s^4-24s^2+8)$	0
1,0	$-144c^2(2-3s^2)^2s^2(15s^2-2)$	$-64c^2(2-3s^2)^2(69s^4-16s^2+6)$	$36c^2(2-3s^2)^2s^2(15s^2-1)$
1,1	$-48c^2(2-3s^2)^2(117s^4-24s^2+8)$	$-12c^2(2-3s^2)^2(1135s^4-448s^2+224)$	$72c^2(2-3s^2)^2s^2(18s^2-1)$
1,2	$-288c^2(2-3s^2)^2(13s^4-12s^2+8)$	$-96c^2(2-3s^2)^2(149s^4-144s^2+80)$	$216c^2(2-3s^2)^2s^4$
1,3	$-768c^2(2-3s^2)^2(3s^4-6s^2+4)$	$-64c^2(2-3s^2)^2(141s^4-224s^2+120)$	0
2,0	$432c^2(2-3s^2)s^2(63s^4-76s^2+16)$	$144c^2(2-3s^2)(399s^6-449s^4+80s^2-8)$	$-27c^2(2-3s^2)s^2(243s^4-274s^2+40)$
2,1	$144c^2(2-3s^2)(375s^6-411s^4+80s^2-8)$	$144c^2(2-3s^2)(883s^6-947s^4+192s^2-40)$	$-216c^2(2-3s^2)s^2(51s^4-56s^2+8)$
2,2	$576c^2(2-3s^2)(36s^6-27s^4+8s^2-8)$	$288c^2(2-3s^2)(223s^6-235s^4+96s^2-40)$	$1296c^4(2-3s^2)s^4$
3,0	$5184c^4s^2(5s^2-2)(6s^2-5)$	$1728c^4s^2(205s^4-239s^2+56)$	$-1296c^4s^2(30s^4-35s^2+8)$
3,1	$3456c^4s^2(4s^2-3)(13s^2-4)$	$1728c^4s^2(261s^4-289s^2+72)$	$2592c^4(2-3s^2)s^2(5s^2-2)$
4,0	$-15552c^6s^2(7s^2-4)$	$-38016c^6s^2(7s^2-4)$	$3888c^6s^2(7s^2-4)$

Table 2
Inclination polynomials $b_{l,k,i,j}$ in Eq. (35); $c = (1 - s^2)^{1/2}$.

i,j	$l = 1, k = 0$	$l = 1, k = 1$	$l = 2, k = 0$
0,0	$8(2-3s^2)^2(3s^4+24s^2-8)$	$6(2-3s^2)^2(3s^4-24s^2+8)$	$-3(2-3s^2)^3$
0,1	$-24(2-3s^2)^2(13s^4-60s^2+20)$	$24(2-3s^2)^2(7s^4-24s^2+8)$	$-6(2-3s^2)^3$
0,2	$-32(2-3s^2)^2(60s^4-123s^2+41)$	$12(2-3s^2)^2(37s^4-72s^2+24)$	$-9(2-3s^2)^3$
0,3	$-8(2-3s^2)^2(399s^4-600s^2+200)$	$24(2-3s^2)^2(15s^4-24s^2+8)$	0
0,4	$-48(2-3s^2)^2(33s^4-48s^2+16)$	0	0
1,0	$24c^2(2-3s^2)s^2(159s^2-68)$	$-12c^2(2-3s^2)(15s^4+212s^2-88)$	$-90c^2(2-3s^2)^2$
1,1	$24c^2(2-3s^2)(207s^4+100s^2-136)$	$24c^2(2-3s^2)(81s^4-384s^2+152)$	$-180c^2(2-3s^2)^2$
1,2	$-72c^2(2-3s^2)(229s^4-368s^2+168)$	$24c^2(2-3s^2)(279s^4-560s^2+200)$	$-216c^2(2-3s^2)^2$
1,3	$-192c^2(2-3s^2)(117s^4-164s^2+60)$	$288c^2(2-3s^2)(15s^4-24s^2+8)$	0
2,0	$-144c^2(552s^6-1087s^4+680s^2-136)$	$96c^2(126s^6-60s^4-127s^2+64)$	$27c^2(2-3s^2)(35s^2-34)$
2,1	$-144c^2(1065s^6-2091s^4+1324s^2-256)$	$192c^2(45s^6+87s^4-217s^2+88)$	$-1728c^4(2-3s^2)$
2,2	$-432c^2s^2(61s^4-61s^2+16)$	$288c^4(57s^4-128s^2+56)$	$-1296c^4(2-3s^2)$
3,0	$864c^4(211s^4-296s^2+100)$	$-1728c^4s^2(22s^2-19)$	$648c^4(7s^2-6)$
3,1	$3456c^4(62s^4-85s^2+32)$	$-1152c^4(27s^4-17s^2-4)$	$-5184c^6$
4,0	$-10368c^6(13s^2-10)$	$6912c^6(5s^2-2)$	$-3888c^6$

tional approach based on the physical time. For the later, the different analytical solutions in the literature for the same truncation order are essentially different arrangements of the same solution, which, therefore enjoy analogous accuracy (Lara, 2021a). However, one formulation may be preferred over others depending on the user needs. Thus, for instance, splitting the solution into additional series may ease coding the solution, but may also increase the computational burden (Lara, 2021c). For our comparisons we choose the approach based on the sequential elimination of the parallax (Deprit, 1981; Lara et al., 2014), the elimination of the perigee (Alfriend and and Coffey, 1984; Lara et al., 2014), and the Delaunay normalization (Deprit, 1982), which seems to be a popular option in the literature (Coffey and Alfriend, 1984; San-Juan, 1994; Coffey et al., 1996; Lara, 2019b). We remark that, unlike in common implementations by different authors, we always improve the initialization of the constants of the traditional perturbation solution with the calibration of the mean semimajor axis from the energy equation (Breakwell and Vagners, 1970).

For the different orbital configurations tested, we always obtained similar comparative results between the traditional and fictitious-time methods. Therefore, we only illustrate them for the PRISMA orbit (Persson et al., 2005), which is a low-eccentricity, sun-synchronous orbit at around 700 km altitude. In particular, in the computation of the initial conditions we used the orbital parameters $a = 6878.14$ km, $e = 0.001, I = 97.42^\circ, \Omega = 168.2^\circ, \omega = 20^\circ$, and $M = 30^\circ$. The true, reference orbit was then computed from the numerical integration of the main problem in Cartesian coordinates. To guarantee that all the stored digits of the reference orbit are exact in the floating-point number representation, the integration was carried out in extended precision. More precisely, we took advantage of the public availability of the implementation by Hairer et al. (2008) of an explicit Runge–Kutta method of order 8(5,3) due to Dormand and Prince (1980), which we compiled in Fortran quadruple precision. The numerical propagations were carried out with tolerance 10^{-22}, and we checked that with our 16-digit truncation of the solution the energy integral and the third component of the angular momentum were both preserved with at least 14 digits (usually 15). In addition, the integration of the fictitious time variation, given by Eq. (2), was incorporated to the differential system in order to check the accuracy provided by each theory exactly at the same physical time.

Results showing the Root Sum Square (RSS) of the errors provided by the first-order truncation of each perturbation solution are shown superimposed in Fig. 1 for a propagation interval of 10 days. The small secular trend in the errors of the traditional solution, of about 1 meter per day, is mostly nullified in the case of the solution based on the extended phase formulation, where the much smaller secular trend remains buried under the periodic oscillations of the errors.

The nature of the position errors of each analytical solution is best illustrated when they are projected in the radial, along-track, and cross-track directions. Indeed, by simple inspection of Fig. 2, we check that the errors in the radial and cross-track directions are periodic in nature and of comparable magnitude in both theories —as it should be expected for perturbation solutions truncated to the same order. On the contrary, while the amplitude of the periodic components of the errors in the along-track direction remain in the case of traditional theory of the same level

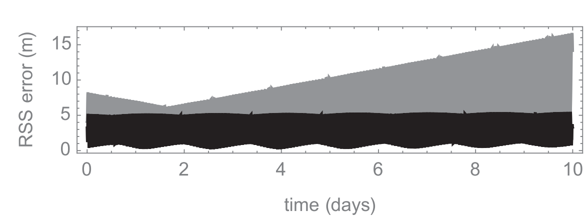

Fig. 1. RSS position errors of the first order theory in the extended phase space (black) superimposed to corresponding errors of the traditional approach (gray).

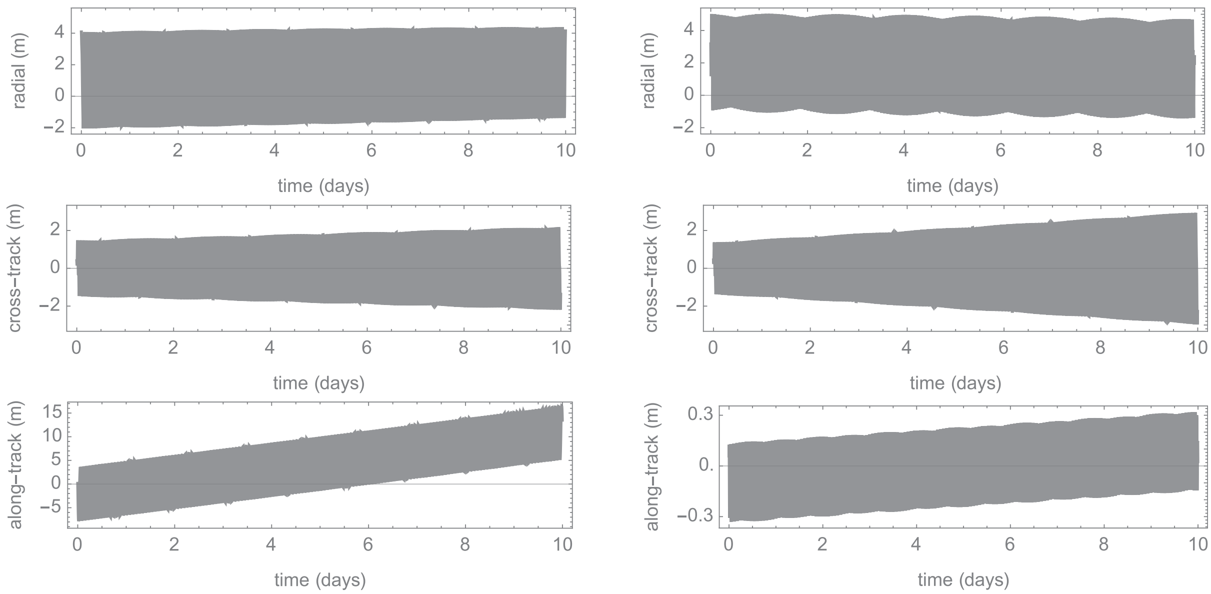

Fig. 2. Intrinsic errors of the first-order traditional (left) and extended phase space theory (right).

of accuracy as the other components of the errors, they reduce by about one order of magnitude, from meters to decimeters, in the case of the extended phase space formulation. The better performance of the extended phase space solution regarding along-track errors applies also to their evident secular component. Visual inspection of the bottom plots of Fig. 2 shows a linear growth of the along-track errors of near 1 m/day for the traditional theory vs. about 10 cm/day in the case of the extended phase space formulation. Given the distinct secular rates, and on account of the already mentioned analogous behavior of the other components of the errors, displayed in the top and center plots of Fig. 2, it becomes evident that along-track errors are mostly responsible of the different behavior of each theory, and the benefits of including the total energy among the integration variables regarding the stabilization of the secular errors in the along-track direction are clearly illustrated.

Undeniably, the greater secular trend of the errors of the traditional solution seems to make the extended phase space solution preferable in much longer propagation times. Still, for actual ephemeris computation, the fictitious time in which the extended phase space solution must be evaluated corresponding to the desired physical time will not be known in advance. On the contrary, its accurate computation requires a root-finding procedure that is commonly approached by Newton–Raphson iterations (Bond, 1979). Moreover, due to the unavoidable truncation of the perturbation solution, the fictitious time corresponding to a given physical time cannot be determined exactly. This issue is not exclusive of analytical perturbation solutions and also emerges in numerical integration schemes based on the fictitious time. While the effect is much more subtle in the latter case, its importance has been clearly recognized and discussed in the literature (Urrutxua et al., 2016). As shown in Fig. 3, the nature of these errors is mostly periodic, with an amplitude of about one half of a millisecond. For the semimajor axis of the PRISMA orbit, this error in the timing may yield an additional in-track error in the meter level. On the other hand, a linear fit to the errors discloses a secular rate of about 10 μs/day, which will clearly show in propagation intervals of just a few weeks.

These additional inaccuracies derived from the $\mathcal{O}(J_2)$ truncation of the series that provide the physical time as a function of the fictitious one, which were not taken into account in Fig. 1, are illustrated in Fig. 4. Now, the errors of the first-order theory in the extended phase space (in black) are true ephemeris errors. That is, they have been computed at given values of the physical time from which the needed fictitious time is obtained by root-finding from the series representing the physical time as an implicit function of the fictitious time. This procedure yields larger errors because the time error of Fig. 3 translates into an additional positional error. The root-finding process

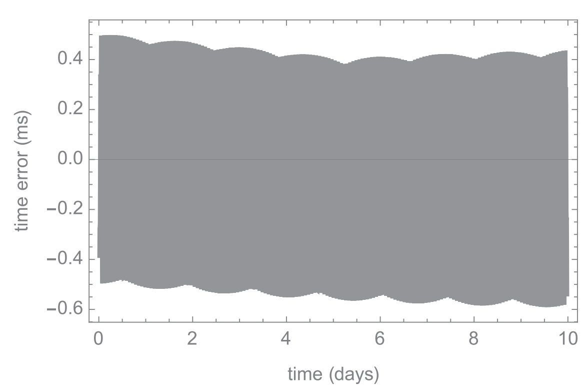

Fig. 3. Errors in the physical time determination stemming from the first-order theory in the extended phase space.

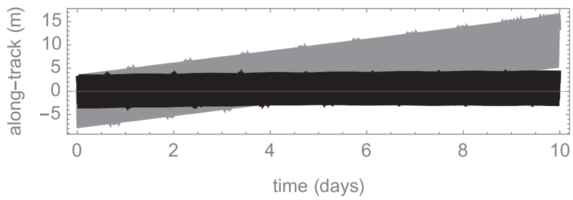

Fig. 4. Along-track errors of the extended phase space theory with the physical time as argument (black) superimposed to the bottom-left plot of Fig. 2.

requires the evaluation of the analytical theory in each iteration, thus notably increasing the computational burden, and, therefore, degrading the performance of the perturbation theory regarding computing time. In the author's coding of the root-finding algorithm, the examples carried out show that the evaluation time needed in each ephemeris evaluation commonly increases by one order of magnitude with respect to the direct evaluation in the fictitious time.

When the second-order theory is used we obtain notable accuracy gains in both cases, as expected from the characteristics of perturbation solutions. Again, the amplitude of the periodic errors in the radial and cross-track directions is similar for both perturbation theories, now in the mm level, and corresponding errors are not presented. On the contrary, while the amplitude of the periodic errors in the along-track direction remains also in the mm level in the case of the solution in extended phase space, it is not at all the case of the errors of the traditional theory, whose amplitude now reaches the cm level. This is shown in Fig. 5, where we also notice the secular rate of the along-track errors of the traditional theory of about one third of cm per day, which is much larger than the rate of about one tenth of mm per day of the extended phase space solution. Nonetheless, these figures yield an analogous ratio to the first-order case.

Again, additional inaccuracies to those presented in Fig. 5 arise in the case of the extended phase space solution due to the need of computing the physical time from the fictitious one, or vice versa. As shown in Fig. 6, the amplitude of these errors is now reduced to about 1 microsecond, which is not enough to hide a clear secular trend of about $0.1\,\mu$s/day. These additional errors of the extended phase space formulation, now reaching the cm level for the PRISMA orbit, result in a notable increase with respect to the mm level shown in the bottom plot of Fig. 5. Again, timing errors notably balance the accuracy of both kinds of theories, as illustrated in Fig. 7. Therefore, like in the first-order case, this source of errors may be a dominant part that cannot be ignored in the performance evaluation of perturbation solutions based on the formulation in the extended phase space. Also like in the first-order case, differences in accuracy will be much more evident in longer time spans due to the distinct secular rates of the along-track errors.

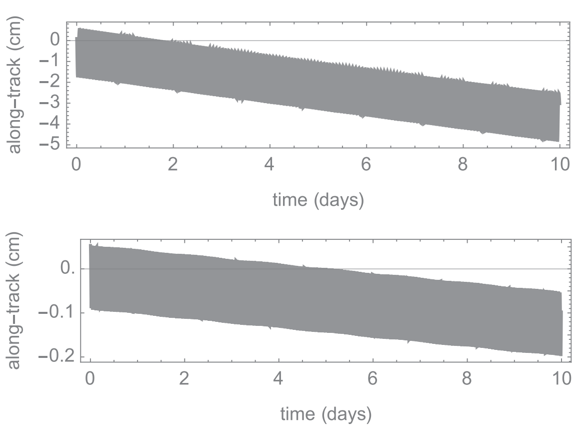

Fig. 5. Along-track errors of the second order theory of the traditional (top) and extended phase space formulation (bottom plot). Note the different scales of the ordinates.

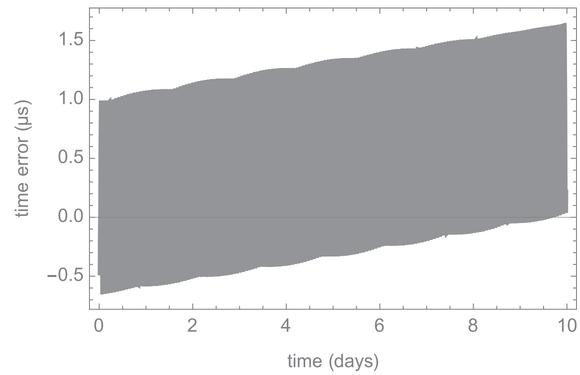

Fig. 6. Errors in the physical time determination stemming from the second-order theory in the extended phase space.

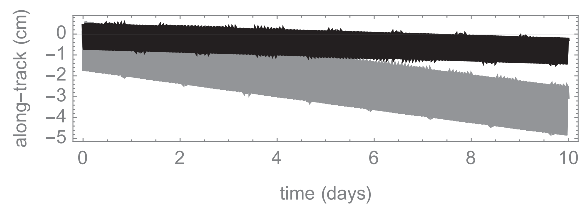

Fig. 7. Along-track errors of the second-order theory in the extended phase space with the physical time as argument (black) superimposed to corresponding errors of traditional theory based on the physical time (gray) previously displayed in the top plot of Fig. 5.

4. Conclusions

Inclusion of the total energy among the variables of an analytic orbit generator has beneficial, radical effects in the propagation of along-track errors of circumterrestrial orbits, which are commonly reduced by one order of magnitude with respect to usual along-track errors obtained with traditional (properly initialized) perturbation solutions. This fact could make the extended phase formulation preferable for mission analysis and planning, as well as end-of-life decommissioning or long-term studies of orbital perturbations. However, this kind of solution has to unavoidably deal with the transformation between physical and fictitious times in ephemeris computation. This is not only a clear inconvenience from the algorithmic point of view, but, most notably, this change cannot be carried out exactly due to the truncation that is inherent to any perturbation solution. Additional inaccuracies stemming from this conversion, which show both secular and periodic trends, may be as important as those derived from the intrinsic components of the position errors. Therefore, they cannot be ignored in the objective assessment of accuracy performance. From the point of view of the construction of the analytical solution, the fictitious-time approach has clear advantages regarding the computation of the integrals involved in the process, yet a post-processing is needed to reduce the length of the series comprising the solution to a comparable size to those resulting from the traditional approach. These pros and cons do not present a clear advantage for one of the options, and make the choice between traditional and extended phase space orbital perturbation solutions mostly a matter of the particular needs of prospective users.

Declaration of Competing Interest

The authors declare that they have no known competing financial interests or personal relationships that could have appeared to influence the work reported in this paper.

Acknowledgments

Partial support by the Spanish State Research Agency and the European Regional Development Fund (Project PID2020-112576 GB-C22, AEI/ERDF, EU) is recognized.

References

Ahmed, M.K.M., 1994. On the normalization of perturbed Keplerian systems. Astron. J. 107, 1900–1903. https://doi.org/10.1086/117001.

Alfriend, K.T., Coffey, S.L., 1984. Elimination of the perigee in the satellite problem. Celestial Mech. 32 (2), 163–172. https://doi.org/10.1007/BF01231123.

Boccaletti, D., Pucacco, G., 2002. Theory of orbits. Volume 2: Perturbative and geometrical methods. In: Astronomy and Astrophysics Library, (1st ed.). Springer-Verlag, Berlin Heidelberg New York.

Bonavito, N.L., Watson, S., Walden, H., 1969. An Accuracy and Speed Comparison of the Vinti and Brouwer Orbit Prediction Methods. Technical Report NASA TN D-5203 Goddard Space Flight Center Greenbelt, Maryland.

Bond, V.R., 1979. An Analytical Singularity-Free Solution to the J_2 Perturbation Problem. Technical Report NASA-TM-58221; JSC-13128 NASA Johnson Space Center.

Breakwell, J.V., Vagners, J., 1970. On Error Bounds and Initialization in Satellite Orbit Theories. Celestial Mech. 2, 253–264. https://doi.org/10.1007/BF01229499.

Brouwer, D., 1959. Solution of the problem of artificial satellite theory without drag. Astron. J. 64, 378–397. https://doi.org/10.1086/107958.

Cain, B.J., 1962. Determination of mean elements for Brouwer's satellite theory. Astron. J. 67, 391–392. https://doi.org/10.1086/108745.

Coffey, S., Alfriend, K.T., 1984. An analytical orbit prediction program generator. J. Guidance, Control Dyn. 7 (5), 575–581. https://doi.org/10.2514/3.19897.

Coffey, S.L., Neal, H.L., Segerman, A.M., Travisano, J.J., 1996. An Analytic Orbit Propagation Program for Satellite Catalog Maintenance. In: Alfriend, K.T., Ross, I.M., Misra, A.K., Peters, C.F. (Eds.), AAS/AIAA Astrodynamics Conference 1995. American Astronautical Society P.O. Box 28130, San Diego, California 92198, USA: Univelt, Inc. volume 90 of Advances in the Astronautical Sciences, pp. 1869–1892.

Deprit, A., 1969. Canonical transformations depending on a small parameter. Celestial Mech. 1 (1), 12–30. https://doi.org/10.1007/BF01230629.

Deprit, A., 1981. A Note Concerning the Tr-Transformation. Celestial Mech. 23 (4), 299–305. https://doi.org/10.1007/BF01230743.

Deprit, A., 1981. The elimination of the parallax in satellite theory. Celestial Mech. 24 (2), 111–153. https://doi.org/10.1007/BF01229192.

Deprit, A., 1982. Delaunay normalisations. Celestial Mech. 26, 9–21. https://doi.org/10.1007/BF01233178.

Deprit, A., Ferrer, S., 1987. Note on Cid's Radial Intermediary and the Method of Averaging. Celestial Mech. 40 (3–4), 335–343.

Deprit, A., Rom, A., 1970. The Main Problem of Artificial Satellite Theory for Small and Moderate Eccentricities. Celestial Mech. 2 (2), 166–206.

Dormand, J.R., Prince, P.J., 1980. A family of embedded Runge-Kutta formulae. J. Comput. Appl. Math. 6 (1), 19–26. https://doi.org/10.1016/0771-050X(80)90013-3.

Eckstein, M.C., Hechler, F., 1970. A reliable derivation of the perturbations due to any zonal and tesseral harmonics of the geopotential for nearly-circular satellite orbits. Scientific Report ESRO SR-13 European Space Research Organisation Darmstadt, Federal Republic of Germany.

Ferrer, S., Lara, M., 2010. Families of Canonical Transformations by Hamilton-Jacobi-Poincaré Equation. Application to Rotational and Orbital Motion. J. Geometric Mech. 2 (3), 223–241. https://doi.org/10.3934/jgm.2010.2.223.

Floría, L., 1997. Perturbed Gylden Systems and Time-Dependent Delaunay-Like Transformations. Celestial Mech. Dyn. Astron. 68 (1), 75–85. https://doi.org/10.1023/A:1008239731649.

Gaias, G., Colombo, C., Lara, M., 2020. Analytical Framework for Precise Relative Motion in Low Earth Orbits. J. Guidance Control Dyn. 43 (5), 915–927. https://doi.org/10.2514/1.G004716.

Hairer, E., Nørset, S.P., Wanner, G., 2008. Solving Ordinary Differential Equations I. Non-stiff Problems, (2nd ed.). Springer-Verlag, Berlin – Heidelberg – New York.

Healy, L.M., 2000. The Main Problem in Satellite Theory Revisited. Celestial Mech. Dyn. Astron. 76 (2), 79–120. https://doi.org/10.1023/A:1008305628985.

Jefferys, W.H., 1971. Automated, Closed Form Integration of Formulas in Elliptic Motion. Celestial Mech. 3, 390–394. https://doi.org/10.1007/BF01231808.

Kozai, Y., 1959. The motion of a close earth satellite. Astron. J. 64, 367–377. https://doi.org/10.1086/107957.

Kozai, Y., 1962. Second-order solution of artificial satellite theory without air drag. Astron. J. 67, 446–461. https://doi.org/10.1086/108753.

Lara, M., 2019a. A new radial, natural, higher-order intermediary of the main problem four decades after the elimination of the parallax. Celestial Mech. Dyn. Astron. 131 (9), 1–20. https://doi.org/10.1007/s10569-019-9921-5.

Lara, M., 2019b. Review of analytical solutions for low earth orbit propagation and study of the precision improvement in the conversion of osculating to mean elements. Technical Report CM 2019/SER0023 Universidad de La Rioja Logroño, La Rioja.

Lara, M., 2020. Solution to the main problem of the artificial satellite by reverse normalization. Nonlinear Dyn. 101 (2), 1501–1524. https://doi.org/10.1007/s11071-020-05857-3.

Lara, M., 2021a. Brouwer's satellite solution redux. Celestial Mech. Dyn. Astron. 133 (47), 1–22. https://doi.org/10.1007/s10569-021-10043-7.

Lara, M., 2021b. Hamiltonian Perturbation Solutions for Spacecraft Orbit Prediction. The method of Lie Transforms volume 54 of De Gruyter Studies in Mathematical Physics. 1st ed., De Gruyter, Berlin/Boston.

Lara, M., 2021c. Improving efficiency of analytic orbit propagation (IAC-21,C1,7,2,x65390). In: Proceedings of the 72nd International Astronautical Congress (IAC), Dubai, United Arab Emirates, 25–29 October 2021. International Astronautical Federation IAF.

Lara, M., San-Juan, J.F., López-Ochoa, L.M., 2014. Delaunay variables approach to the elimination of the perigee in Artificial Satellite Theory. Celestial Mech. Dyn. Astron. 120 (1), 39–56. https://doi.org/10.1007/s10569-014-9559-2.

Lara, M., San-Juan, J.F., López-Ochoa, L.M., 2014b. Proper Averaging Via Parallax Elimination (AAS 13–722). In: Broschart, S.B., Turner, J. D., Howell, K.C., Hoots, F.R. (Eds.), Astrodynamics 2013. American Astronautical Society P.O. Box 28130, San Diego, California 92198, USA: Univelt, Inc. volume 150 of Advances in the Astronautical Sciences. pp. 315–331.

Lyddane, R.H., 1963. Small eccentricities or inclinations in the Brouwer theory of the artificial satellite. Astron. J. 68 (8), 555–558. https://doi.org/10.1086/109179.

Lyddane, R.H., Cohen, C.J., 1962. Numerical comparison between Brouwer's theory and solution by Cowell's method for the orbit of an artificial satellite. Astron. J. 67, 176–177. https://doi.org/10.1086/108689.

Metris, G., 1991. Mean values of particular functions in the elliptic motion. Celestial Mech. Dyn. Astron. 52, 79–84. https://doi.org/10.1007/BF00048588.

Persson, S., Jacobsson, B., Gill, E., 2005. PRISMA – Demonstration Mission for Advanced Rendezvous and Formation Flying Technologies and Sensors (paper IAC-05-B56B07). In: Proceedings of the 56th International Astronautical Congress (IAC). International Astronautical Federation, Fukuoka, Japan, pp. 1–10.

Poincaré, H., 1893. Les méthodes nouvelles de la mécanique céleste. Tome 2. Gauthier-Villars et fils (Paris).

San-Juan, J.F., 1994. ATESAT: Automatization of theories and ephemeris in the artificial satellite problem. Technical Report CT/TI/MS/MN/94-250 Centre National d'Études Spatiales 18, avenue Edouard Belin - 31401 Toulouse Cedex 9, France.

Scheifele, G., 1970. Généralisation des éléments de Delaunay en mécanique céleste. Application au mouvement d'un satellite artificiel. Academie des Sci. Paris Comptes Rendus Serie B Sci. Phys. 271, 729–732.

Scheifele, G., 1970. On Nonclassical Canonical Systems. Celestial Mech. 2 (3), 296–310. https://doi.org/10.1007/BF01235123.

Scheifele, G., 1981. An analytical singularity-free orbit predictor for near-earth satellites. In: Proceedings of the International Symposium on Spacecraft Flight Dynamics, Darmstadt, 18–22 May 1981. volume 160 of ESA Special Publication. pp. 299–305.

Scheifele, G., Graf, O., 1974. Analytical satellite theories based on a new set of canonical elements. In: Mechanics and Control of Flight Conference. American Institute of Aeronautics and Astronautics, Reston, Virigina, pp. 1–20. https://doi.org/10.2514/6.1974-838.

Stiefel, E.L., Scheifele, G., 1971. Linear and Regular Celestial Mechanics volume 174 of Grundlehren der mathematischen Wissenschaften. 1st ed., Springer-Verlag, Berlin Heidelberg.

Urrutxua, H., Peláez, J., Bombardelli, C., 2016. Impact of the integration stop-condition on the accuracy of regularized orbit formulations (AAS 16–353). In: Ozimek, M.T. Zanetti, R.,Russell, R. P., Bowes, A.L., (Eds.), Spaceflight Mechanics 2016, Part-I. American Astronautical Society, P.O. Box 28130, San Diego, California 92198, USA: Univelt, Inc. volume 158 of Advances in the Astronautical Sciences. pp. 2503–2516.

Ustinov, B.A., 1967. Motion of Satellites in Small-Eccentricity Orbits in the Noncentral Gravitational Field of the Earth. Cosm. Res. 5, 159–168.

Walter, H.G., 1967. Conversion of osculating orbital elements into mean elements. Astron. J. 72, 994–997. https://doi.org/10.1086/110374.